

DAMPING: A SENSITIVE STRUCTURAL PROPERTY FOR DAMAGE DETECTION

Curadelli, R. O.^a, Riera, J.D.^b, Ambrosini, R.D.^a and Amani, M.G.^a

^aGrupo de Dinámica Experimental, Universidad Nacional de Cuyo, Parque Gral San Martín Centro Universitario, Mendoza, Argentina, ocuradelli@fing.uncu.edu.ar, <http://www.fing.uncu.edu.ar>

^bLaboratorio de Dinámica y Confiabilidad, Universidad Federal de Río Grande do Sul, Porto Alegre, Brasil, riera@cpgec.ufrgs.br, <http://www.ufrgs.br>

Keywords: Structural damage, Modal damping, Identification of modal parameters

Abstract. Data from vibration measurements opens a way to damage assessment by correlating changes in system dynamic parameters with damage indicators. Most methods proposed in the literature are based on the measurement of natural frequencies or modal shapes and modelling damage as local reduction in structural stiffness. In some particular applications these methods, however, have several practical limitations on account of their low sensitivity to damage. This paper shows that damping can be used as a damage-sensitive system property and presents a procedure for instantaneous natural frequencies and damping identification from free vibration response using the wavelet transform. Experimental and simulated examples show that in the structures analyzed damage causes important variations of damping parameters.

1 INTRODUCTION

The interest in structural monitoring and damage detection is shared by the civil, mechanical and aerospace engineering communities. Current damage-detection methods are visual or localized experimental procedures such as acoustic or ultrasonic methods, magnet field methods, radiographs, eddy-current and thermal field methods. All these experimental techniques require that the location of damage be known a priori and that the portion of the structure being inspected be easily accessible. These limitations led to the development of global monitoring techniques based on changes in the vibration characteristics of the structure.

Damage or fault detection, by monitoring changes in the dynamic properties or response of the structure, has received considerable attention in recent literature. The basic idea springs from the notion that modal parameters (notably frequencies, mode shapes, and modal damping) are functions of the physical properties of the structure (mass, damping, and stiffness). Therefore, changes in the physical properties will cause changes in the modal properties. Literature reviews on damage identification and health monitoring of structures based on changes in their measured dynamic properties may be found, for example, in [Doebling et al. \(1996, 1998\)](#), [Zou et al. \(2000\)](#), [Sohn et al. \(2003\)](#), [Salawu, \(1997\)](#) and [Chang et al. \(2003\)](#).

Structural damage usually results in a decrease in mass, stiffness and strength of structural elements. In consequence, its detection and localization have great practical importance and led to the development of a research field rather incorrectly known as *Structural Health Monitoring* (SHM) ([Chang, 1999](#)) since it would sound awkward to qualify any structure as *healthy*. At any rate, four SHM categorical levels were proposed to quantify damage in Engineering Structures: Level 1: damage detection; Level 2: damage location; Level 3: quantification of the degree of damage; Level 4: estimation of the remaining service life. For such purpose, one of the most frequently used SHM techniques are vibration-based methods ([Rytter, 1993](#)).

Vibration methods are based on the observation that the presence of damage in a structure produces a local increase in flexibility, which induces changes in its dynamic properties. These changes can be used for damage identification.

The amount of literature related to damage detection using shifts in natural frequencies is quite large. The forward problem, which usually falls into the category of Level 1 damage identification, consists of calculating frequency shifts for a known type of damage. Typically, damage is modelled numerically by a reduction in the stiffness and then the measured frequencies are compared to the frequencies predicted by the model. Moreover, this technique is used extensively in damage diagnosis and health monitoring of existing highway bridges, seismic behaviour and residual capacity of structures.

It should be noted that frequency shifts have some practical limitations in several applications, especially in case of large structures ([Farrar et al, 1994](#), [Doebling et al, 1996](#) and [Sohn et al, 2003](#)), although ongoing research may help circumvent these difficulties. The usually small frequency shifts caused by damage require either very precise measurements or high levels of damage.

Damping properties, on the other hand, have rarely been used for damage diagnosis. Crack detection in a structure based on damping, however, has advantages over detection schemes based on frequencies and modal shapes. In fact, damping changes may render the detection of the nonlinear, dissipative effects that cracks produce feasible, while cracks usually lead to small or no frequency variations. [Modena, Sonda and Zonta \(1999\)](#) show that visually undetectable cracks cause very little change in resonant frequencies and require higher mode

shapes to be detected, while these same cracks cause larger changes in damping. In some cases, damping changes of around 50% were observed. Their study focuses on identifying manufacturing defects or structural damage in precast reinforced concrete elements. The particular dynamic response of reinforced concrete justifies the use of damping as a damage-sensitive property, proposing two new methods based on changes in damping to detect cracking. These techniques are employed to locate cracks in a 1.20×5.80 m precast hollow floor panel excited with stepped sines and shocks, and the diagnosis results are compared with those of frequency and curvature based approaches.

Kawiecki (2000) measures damping in a $90 \times 20 \times 1$ mm metal beam and metal blanks used to fabricate 3.5-in. computer hard disks, noting that damping can be a useful damage-sensitive indicator. Modal damping is determined using the half-power bandwidth method applied to the FRF within the frequency range of 5 kHz to 9 kHz obtained from measured data. Kawiecki (2000) claims that the approach should be particularly suitable for structural health monitoring of lightweight and microstructures.

After conducting prestressed reinforced concrete hollow panels vibration tests, Zonta et al, (2000) observe that cracking produces a frequency splitting in the frequency domain and the beat phenomenon of the free decay signals in the time domain. It is argued that crack formation in prestressed reinforced concrete causes a nonviscous dissipative mechanism, making damping more sensitive to damage, and they propose to use this dispersive phenomenon as a feature for damage diagnosis. Zonta et al. (2000) point out that the dispersive phenomenon cannot be represented by the standard linear model of a single degree of freedom system and emphasize that the oscillator has a variable stiffness, and this variability is proportional to the frequency. They recognize the need for further research using the dispersion phenomenon for damage detection because additional effects such as hysteresis and other nonclassical dissipative mechanisms must be considered.

In large civil engineering structures it is usually unfeasible to measure all components of the input excitation. Experimental modal identification through ambient vibration response records has consequently become a very attractive technique. Within this context, this paper discusses the changes in modal frequencies and damping on structures progressively damaged, applying the wavelet transform. Because the wavelet estimation technique requires free decay response observations, which is rarely feasible on large structures, the modal identification herein proposed is indeed an appealing technique. Ambient excitations such as traffic or wind have the advantage that no equipment is needed to excite the structure. To convert ambient random response to free decay responses the well established *Random Decrement Technique* was used.

2 INTRODUCTION TO IDENTIFICATION OF MODAL FREQUENCIES AND DAMPING

Although various complex phenomena occur when different materials / structural members are damaged, principally under seismic excitation, only two are commonly associated with damage: stiffness and strength deterioration. Hence most models describing the hysteretic behaviour of structural members have been derived from the shape of experimental force-displacement relationship (hysteretic curves). Examples of macro models proposed to represent this complex behaviour are Takeda-type (Takeda et al. 1970) and their variations (Tang and Goel, 1988 and Hueste and Wight, 1999), which simulate phenomena such as stiffness and strength degradation and pinching in concrete beams and columns. An oscillator with this type of behaviour can be approximated by second-order systems with nonlinear

restoring force $k(x)x$ and nonlinear damping force $h(\dot{x})\dot{x}$ and represented by the equation $\ddot{x} + 2h_o(\dot{x})\dot{x} + k(x)x = 0$, which leads to a free response of the form:

$$x(t) = A(t) \cos(\varphi(t)) \quad (1)$$

Note that functions h_o and k represent apparent (viscous) damping and apparent (elastic) stiffness coefficients, respectively. In the following they will be referred to simply as damping and stiffness coefficients. In the identification technique, the envelope $A(t)$ (instantaneous amplitude) and the instantaneous phase $\varphi(t)$ or the instantaneous angular frequency $\omega(t) = \dot{\varphi}(t)$, can be extracted from the vibration signals employing the wavelet transform, as described in appendix A. (Chuang and Chen, 2003, 2004; Lu and Hsu, 2002; Wang and Deng, 1999; Minh-Nghi and Lardies, 2006; Lardies and Gouttebronze, 2002; Kim and Melhem, 2004). Feldman (1994, 1997) showed, by applying the multiplication property of the Hilbert Transform for overlapping functions to the equation of motion for viscous damping systems, that the instantaneous undamped natural frequency and the instantaneous damping coefficient may be calculated according to the formulas:

$$\omega_o^2(t) = \omega^2 - \frac{\ddot{A}}{A} + \frac{2\dot{A}^2}{A^2} + \frac{\dot{A}\dot{\omega}}{A\omega} \quad , \quad (2)$$

$$h_o(t) = -\frac{\dot{A}}{A} - \frac{\dot{\omega}}{2\omega}$$

where $\omega_o(t)$, is the instantaneous undamped natural frequency and $h_o(t)$ the instantaneous damping coefficient of the system. $A(t)$ and $\omega(t)$ are the envelope (instantaneous amplitude) and the instantaneous angular frequency of the vibratory system solution with their first and second time derivatives $(\dot{\omega}, \dot{A}, \ddot{A})$. These two equations establish an identification technique to determine the undamped natural frequency and damping parameters of the systems as instantaneous functions of time at every point of the vibration process. Employing this procedure, the evolution of the system parameters with increasing damage will be analyzed in several illustrative examples.

3 CHANGES IN FREQUENCY AND DAMPING WITH DAMAGE

In non-linear systems (non-linear dissipative and elastic forces) the damping coefficient and the natural frequency become functions of the vibration amplitude. With the aim of determining the evolution of the system parameters (natural frequency and damping coefficient) with vibration amplitude and increasing damage, four examples were analyzed.

3.1 The bilinear oscillator

The simple hysteretic bi-linear model (elastic and elasto-plastic spring and damper) shown in Figure 1 will be considered first. In order to simulate low levels of damage, three cases with different yield force and post-yield to initial stiffness ratio were considered. Table 1 presents the yield force and the ratio between post-yield and initial stiffness in each case. The yield displacement was taken equal to one millimetre, while an additional internal viscous damping equal to 0.5% was adopted in all cases. The system motion analyzed in the following is the free vibration ensuing an initial displacement 5 times larger than the yield displacement.

| Case | Yield Force (fraction of total weight) [%]* | Post to pre-yield stiffness ratio [%] |
|------|--|--|
| 1 | 5 | 99 |
| 2 | 15 | 97 |
| 3 | 25 | 95 |

Table 1. System parameters for cases 1 to 3.

* Yield displacement $d_y = 1\text{mm}$, initial displacement = $5 d_y$

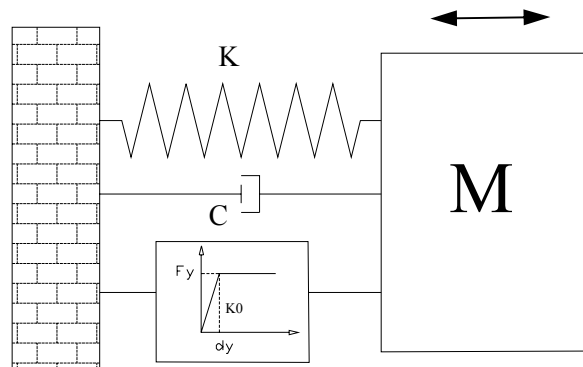
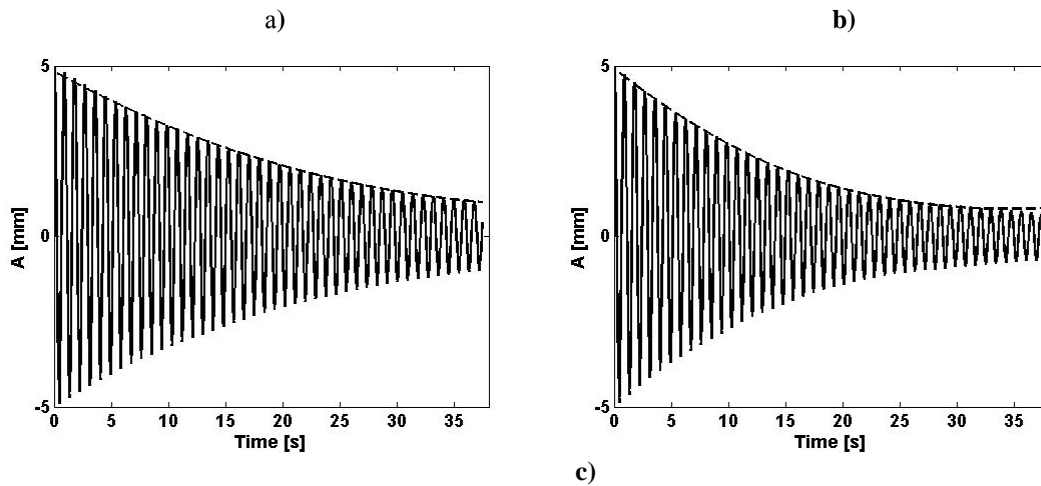


Figure 1. Non linear (bilinear) oscillator (Cases 1 to 3).

In Figure 1, F_y denotes the yield force, d_y the yield displacement, $K + K_0$ the initial stiffness and K the post-yield stiffness. Figures 2 (a-c), show the free vibration response and the envelope determined by the identification technique.



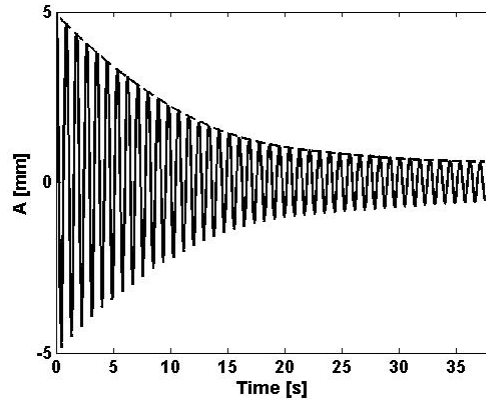


Figure 2. Free vibration response and envelope. (a) case 1, (b) case 2, (c) case 3.

Figure 3 shows the dependence of the *instantaneous* natural frequency on the instantaneous amplitude of vibration, which represents a kind of skeleton (or backbone) curve of the system. Figure 4 shows the dependence of the instantaneous damping coefficient on the instantaneous vibration amplitude.

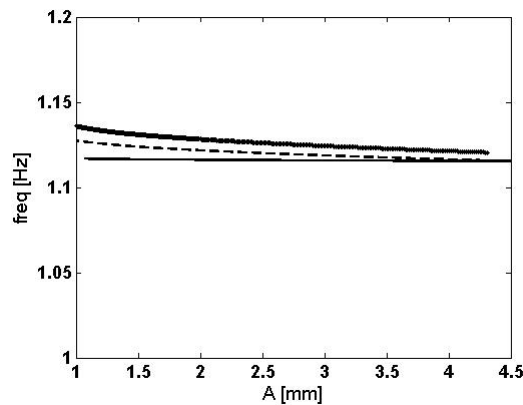


Figure 3. Instantaneous undamped natural frequency vs instantaneous amplitude. (Backbone curves)
Cases: — 1, - - - 2, ——— 3.

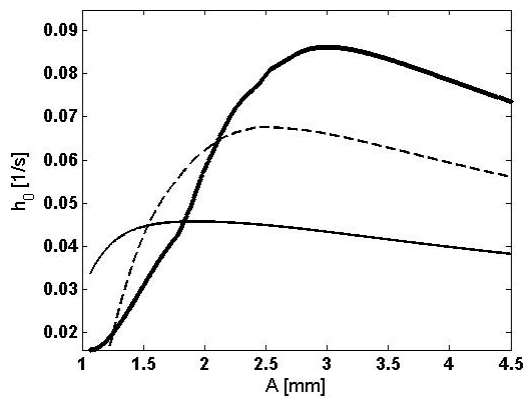


Figure 4. Instantaneous damping coefficient vs instantaneous amplitude.
Cases: — 1, - - - 2, ——— 3.

Figure 3 shows that the *instantaneous* undamped natural frequency has a minor change due to the low degree of damage considered. However, figure 4 shows that damping changes

significantly. It seems quite clear than in this case damping could be advantageously used as a damage indicator because it is more sensitive to damage than the instantaneous frequency. However, it is probable that the statistical variations of natural frequencies are lower than the damping. It is important to point out that the relationship between instantaneous frequency and vibration amplitude and between instantaneous damping coefficient and vibration amplitude are similar to those obtained earlier by harmonic linearization of a bilinear oscillator (Curadelli, 2003).

3.2 Numerical simulation of the response of 2D reinforced concrete frame with strength and stiffness degradation

In order to assess changes in the system parameters caused by damage in a more complex structure, a 2D reinforced concrete frame modelled with inelastic elements described by constitutive rules capable of representing hysteresis stiffness degradation and pinching was analyzed next. The example is a three bays, six-stories high reinforced concrete frame, designed for a PGA of 0.17 g (value from a seismic hazard curve that presents a 10% probability of exceedance in 50 years), in accordance with the provisions of the Argentine Code INPRES-CIRSOC 103 or ACI, which in this case result in similar designs (Curadelli and Riera, 2004). The total mass per floor is 100t, Young’s modulus of concrete $E = 24.8$ GPa which lead to a fundamental period $T_1 = 1$ s. The internal damping ratio was assumed equal to 5% of critical. In the non-linear constitutive relations, the yield strength of reinforcing steel and the compressive strength of concrete were assumed equal to $f_y = 413$ MPa and $f_c = 27.6$ MPa, respectively. Figure 5 shows the basic dimensions of the frame.

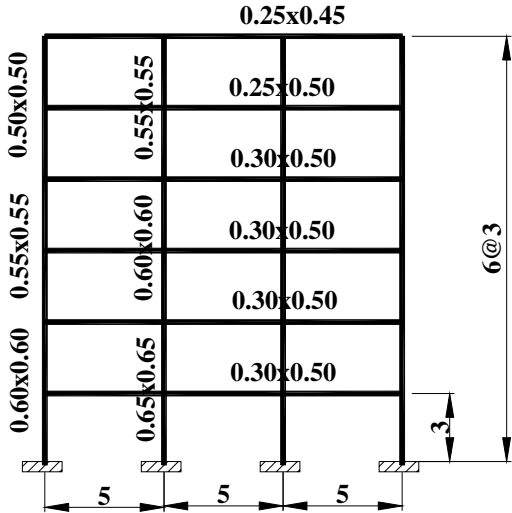


Figure 5. Reinforced concrete 2D frame structure.

The structure was submitted to the Caucete, San Juan, Argentina 1997 seismic acceleration time history. From the last 10 s of the roof response, which is actually a free vibrations record, changes in the system parameters were determined by the procedure described above. In order to assess different degree of structural damage, the accelerograms were normalized to four intensity levels (1, 2, 3 and 4m/s^2 (collapse)), defined in terms of their PGA.

Figures 6a and 6b show the free response and the corresponding envelopes, determined by the identification technique, for the first and ultimate degrees of damage.

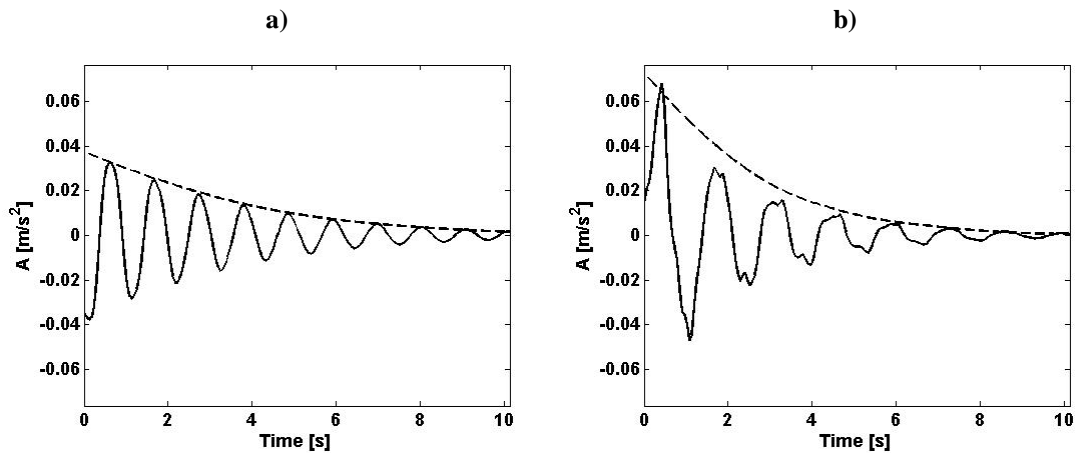


Figure 6. Free vibration response and envelope. (a) first and (b) ultimate degree of damage of 2D Frame Structure.

Figures 7 and 8 show the dependence of the *instantaneous* fundamental frequency and instantaneous damping coefficient on the amplitude of vibration, respectively, for each damage level.

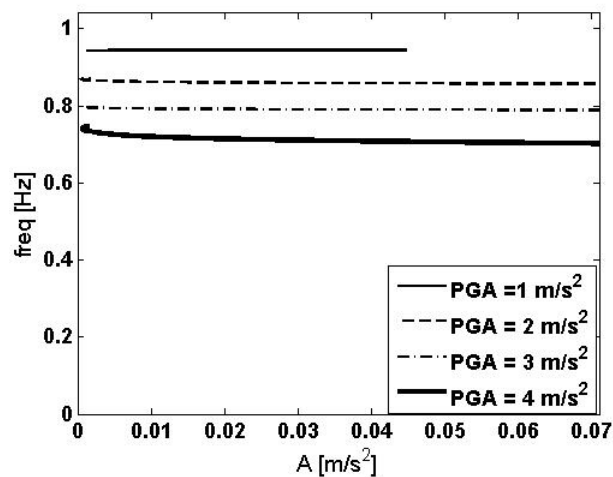


Figure 7. Instantaneous undamped fundamental frequency vs. instantaneous vibration amplitude.

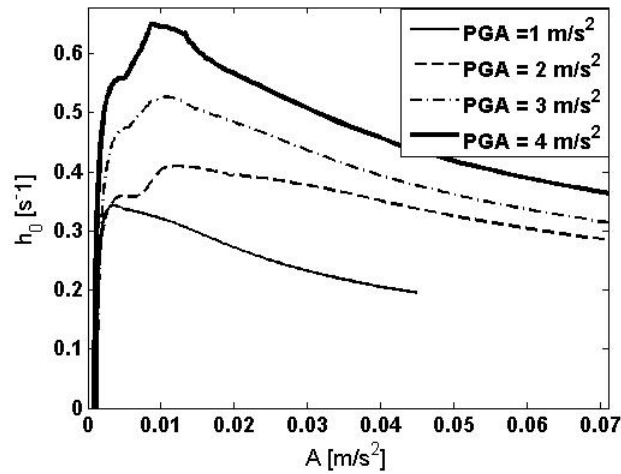


Figure 8. Instantaneous damping coefficient vs instantaneous amplitude of vibrations.

Figures 7 and 8 provide valuable evidence on the influence of damage on dynamic properties of the reinforced concrete frame. The maximum undamped fundamental frequency reduction, observed for a 0.4g PGA, reaches nearly 25%, increasing linearly with the PGA. Damping, on the other hand, presents more pronounced and typical variations.

3.3 Experimental study of reinforced concrete beam

The performance of the identification procedure was also assessed using experimental data, for which purpose a reinforced concrete beam tested by Palazzo (2000) was analyzed. The specimen was a 0.20 m × 0.10 m × 5.60 m reinforced concrete beam in flexure under two points loading (figure 9a and b). The yield strength of reinforcing steel bars and the compressive strength of concrete were $f_y = 420$ MPa and $f_c = 17$ MPa, respectively. Loads were increased monotonically until the intensities indicated in Table 2 were reached, as schematically shown in Figure 10. At that point loads were removed and free vibration tests conducted to determine dynamic properties. The procedure was then repeated for the next loading step. Figure 11 (a-b) shows the observed free vibration response after the first and the last loading step, respectively.

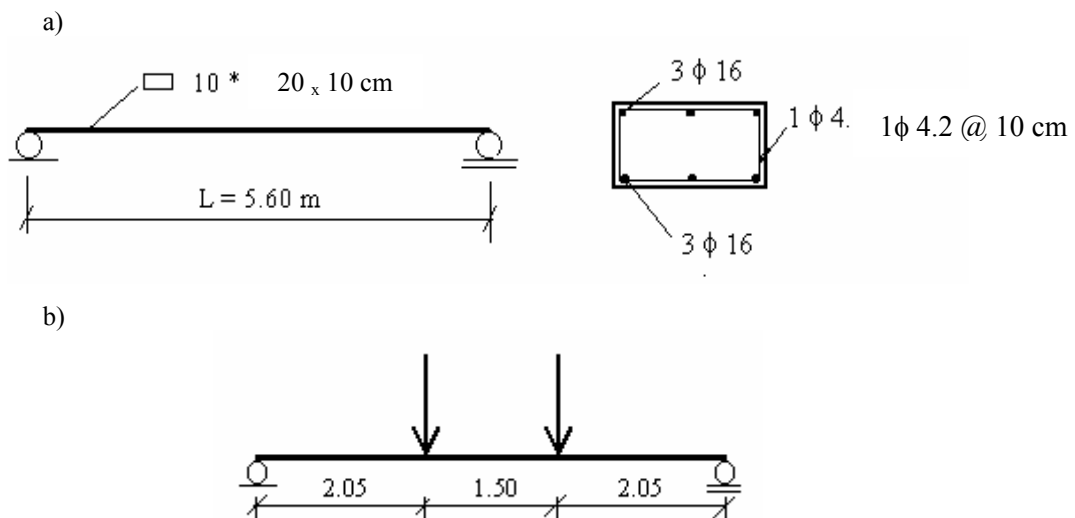


Figure 9 (a) Sketch of reinforced concrete simply supported beam tested (b) load location.

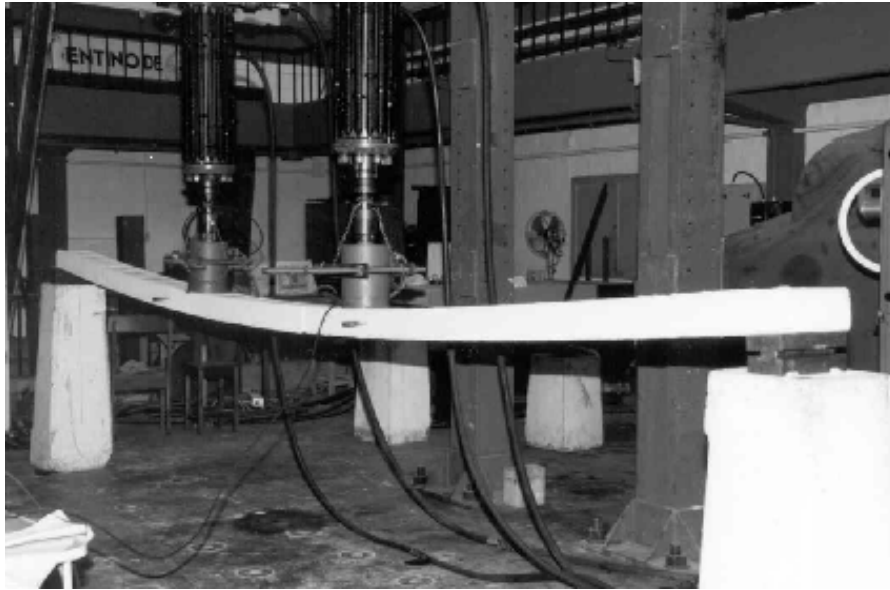


Figure 10. Reinforced concrete beam test setup.

| Load step | Load [kN] | Fundamental frequency measured after each load step |
|-----------|------------|---|
| 0 | 0 | 4.55 |
| 1 | 2 x 1,46 | 4.34 |
| 2 | 2 x 2,25 | 4.29 |
| 3 | 2 x 3,23 | 4.25 |
| 4 | 2 x 5,19 | 4.01 |
| 5 | 2 x 7,25 * | 3.81 |

Table 2. Load step values (from Palazzo, 2000)

* Maximum load considered (correspond to 3.5 ‰ , maximum compress strain, [INPRES-CIRSOC 201](#))

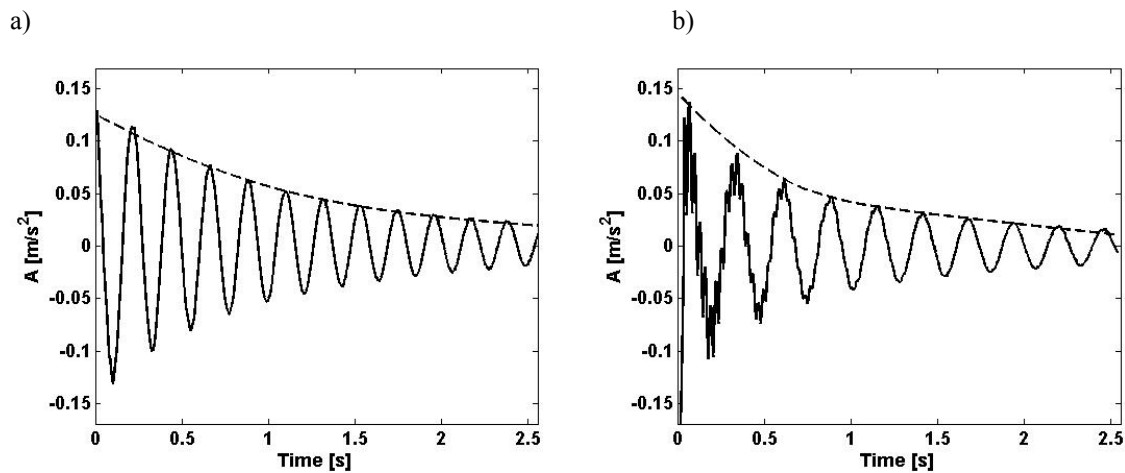


Figure 11. Free vibration response and his envelope after: (a) Test after load step 1 and (b) test after load step 5. (Palazzo, 2000).

The correlation between the instantaneous fundamental frequency and instantaneous damping coefficient and the amplitude of vibration, for the damage condition after Load Step 1 and after Load Step 5, is presented in Figure 12 and 13, respectively.

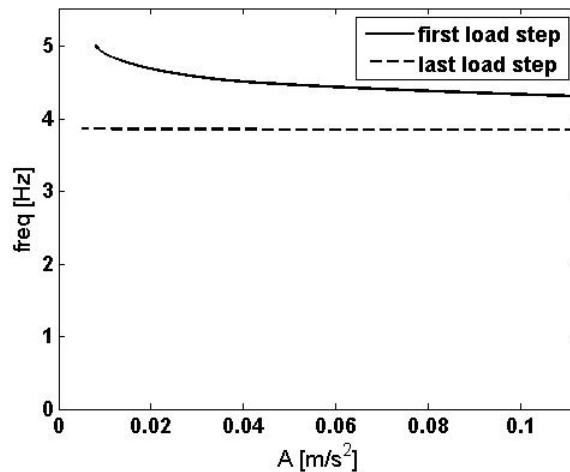


Figure 12. Instantaneous undamped fundamental frequency vs instantaneous amplitude of vibrations.

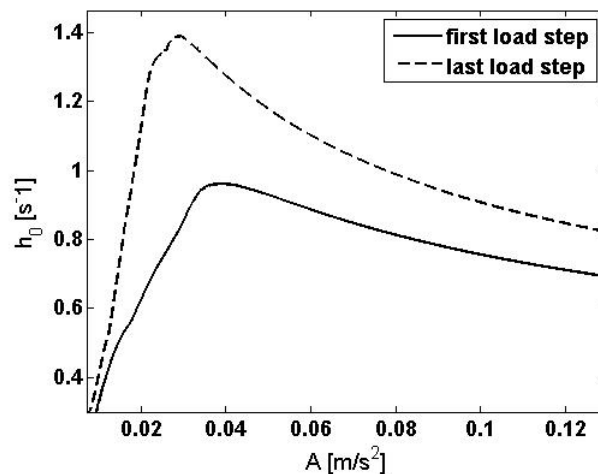


Figure 13. Instantaneous damping coefficient vs instantaneous amplitude of vibrations.

Figures 12 and 13 show the *instantaneous* modal parameters along time for two different level of damage. It is clear that damping has an important variation.

3.4 Experimental 3D frame model

As second experimental example, the one bay, six-storeys high aluminium 3D frame model tested by Amani (2007) was analyzed (Figure 14). Geometric properties are indicated in Table 3 (more details are reported in Amani, 2004). Structural damage was caused by subjecting the model to a horizontal unidirectional base motion in a shaking table. The excitation consisted of a series of 9 simulated acceleration time histories (Gaussian white noise) with increasing intensity. The standard deviations of the base acceleration in the tests were $\sigma_a = 1.8; 2.1; 6.1; 12; 20; 32; 38; 44; \text{ and } 48 \text{ m/s}^2$. As it was mentioned before, the wavelet transform procedure for modal parameters identification operates on the free

vibration. Thus, in order to obtain free decay response, the measured horizontal acceleration response at top floor was processed by *random decrement technique* (Ibrahim, 1986, Ibrahim et al, 1996). Follow figures show the changes of investigated parameter along time for both, lowest excitation level ($\sigma_a = 1.8 \text{ m/s}^2$, undamaged) and highest excitation level ($\sigma_a = 48 \text{ m/s}^2$, severe damage).

| | | |
|-----------------------|------------|------------------------|
| Total height | | 0.50 m |
| Story height | | 0.083 m |
| Span length | | 0.10 m |
| Columns cross section | Stories1&2 | 0.6 x 18 (mm) |
| | Stories3&4 | 0.6 x 12 (mm) |
| | Stories5&6 | 0.6 x 6 (mm) |
| Total mass | | 0.665kg |
| Mass density | | 2698 kg/m ³ |
| Young's modulus | | 67 GPa |

Table 3. Geometrical and mechanical properties of the model.



Figure 14. One bay, six-storeys high aluminum 3D frame model tested by Amani 2007.

Figure 15 a-b show measured free vibration acceleration response at top floor obtained from *random decrement technique* for the lowest and highest excitation level, respectively.

a)

b)

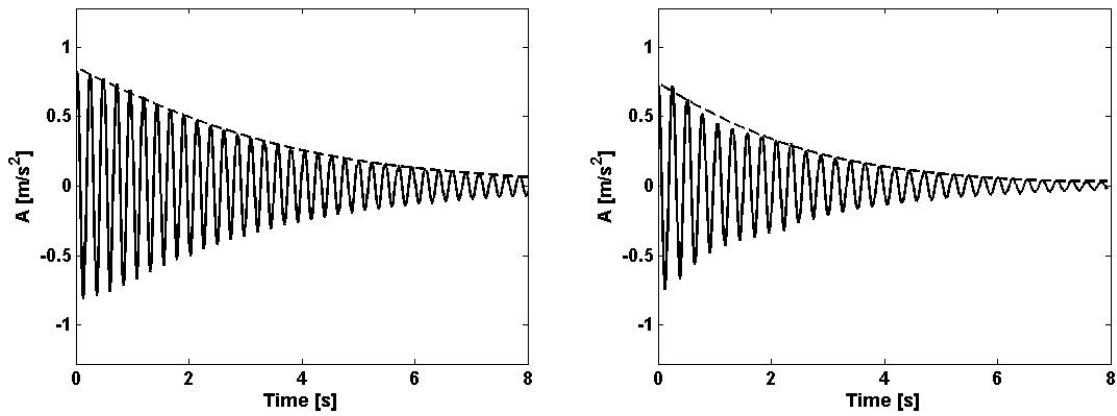


Figure 15. Free vibration acceleration response and the envelope for: a) lowest and b) highest excitation level. One bay, Six-storeys high aluminium 3D frame model tested by [Amani 2007](#).

Figure 16 and 17 show the dependence of *instantaneous* fundamental frequency and instantaneous damping coefficient on the instantaneous amplitude of vibrations, respectively, for the lowest and highest excitation level, respectively.

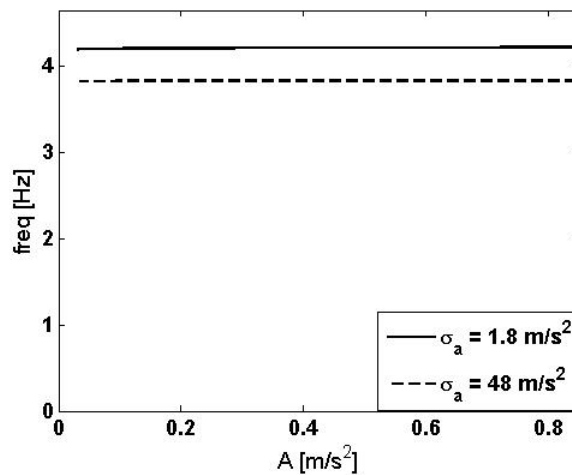


Figure 16. Instantaneous undamped fundamental frequency vs instantaneous amplitude of vibrations.

- $\sigma_a = 1.8 \text{ m/s}^2$, undamaged),
- - - $\sigma_a = 48 \text{ m/s}^2$, severe damage)

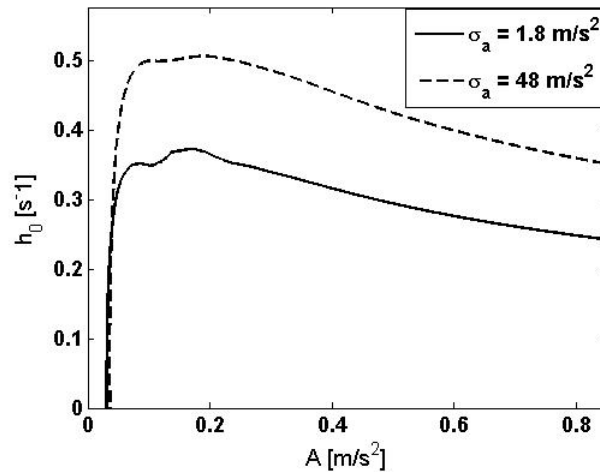


Figure 17. Instantaneous damping coefficient vs instantaneous amplitude of vibrations.

— lowest excitation level ($\sigma_a = 1.8 \text{ m/s}^2$, undamaged),
 - - - highest excitation level ($\sigma_a = 48 \text{ m/s}^2$, severe damage)

Similarly, figures 16 and 17 show that increasing excitation yield to a damage level reducing the undamped fundamental frequency about 9%, while damping reveal more marked variations.

4 CONCLUSIONS

For the kind of structures analyzed, damage detection technique using damping, as sensitive-damage feature, has shown that is potentially useful. It seems quite clear than; in systems as analyzed, damping is a promising damage indicator in structural health monitoring because it has more sensibility to damage than the natural frequency. However, it is likely that the statistical variations of natural frequencies are lower than the damping. The paper also describes an approach, based on wavelet transform, to determine *instantaneous* natural frequencies and damping from free vibration response of the non-linear systems.

With examples using experimental results and numerical simulation on structures subjected to seismic base excitation it was demonstrated that the identification technique based on wavelets is useful to assess changes in the vibration characteristics due to incremental damage of non-linear systems.

It is also stressed that this work is a start point for damage identification based on damping measurement, and it is needed further research in the subject.

Acknowledgements

The authors wish to thank the financial aid of CONICET, Argentina and CNPq and CAPES, Brazil.

REFERENCES

- Amani, MG. Identificación de Sistemas y Evaluación del Daño Estructural, *PhD thesis* Nacional University of Tucumán, Argentina, 2004.
- Amani, M.G., Riera, J. and Curadelli, O., Identification of changes in the stiffness and damping matrices of linear structures through ambient vibrations, *Journal of Control and Health Monitoring*, 2007 (in press).
- Chang F.K., Structural health monitoring 2000, *Proceedings of the Second International*

- Workshop on SHM*, Stanford, 1999.
- Chang P. C. Flatau, A. and Liu, S. C. Review Paper: Health Monitoring of Civil Infrastructure, *Structural Health Monitoring*, 2, 3: 257-267, 2003.
- Chuang C.C, Chen L.W., Damage detection of a rectangular plate by spatial wavelet based approach, *Applied Acoustics*, 65: 819–832, 2004.
- Chuang C.C, Chen L.W., Vibration damage detection of a Timoshenko beam by spatial wavelet based approach, *Applied Acoustics*, 64: 1217–1240, 2003.
- Chui C.K., Wavelets analysis and Applications: *An Introduction to Wavelets*, Academic Press, New York, 1992.
- Curadelli, R.O. Controle de vibrações em estruturas usando amortecedores metálicos, *PhD thesis*, Federal University of Rio Grande do Sul, Brazil(in portuguese), 2003.
- Curadelli, R. O. and Riera J. D. Reliability based assessment of the effectiveness of metallic dampers in buildings under seismic excitations, *Engineering Structures*, 26: 1931–1938, 2004.
- Doebling, S.W., Farrar Ch., Prime M.B., Shevitz D.W., Damage Identification and Health Monitoring of Structural and Mechanical Systems from Changes in Their Vibration Characteristics: A Literature Review. *Los Alamos National Laboratory Report, LA-13070-MS, UC900*, 1996.
- Doebling, S. W., Farrar, C. R. and Prime, M. B., A Summary Review of Vibration-Based Damage Identification Methods”, *Shock and Vibration Digest*, 30: 91–105, 1998.
- Farrar, C.R., W.E. Baker, T.M. Bell, K.M. Cone, T.W. Darling, T.A. Duffey, A. Eklund, and A. Migliori, , Dynamic Characterization and Damage Detection in the I-40 Bridge Over the Rio Grande, *Los Alamos National Laboratory report LA-12767-MS*, 1994.
- Feldman M, Non-linear free vibration identification via the Hilbert transform, *Journal of Sound and Vibration*, 208, 3: 475–489, 1997.
- Feldman M., Non-linear free vibration analysis using Hilbert transform – I. Free vibration analysis method “freevib”, *Mechanical Systems and Processing*, 8, 2: 119–127, 1994.
- Hueste, M. B. D. and J. K., Wight, Nonlinear Punching Shear Failure Model for Interior Slab-Column Connections, *Journal of Structural Engineering*, ASCE, 125, 9: 997-1008, 1999.
- Ibrahim S.R., Incipient failure detection from random decrement time functions, *International Journal of Analytical and Experimental Modal Analysis*, 1: 1-8, 1986.
- Ibrahim S.R., Brincker R., and Asmussen J., Modal parameter identification from responses of general unknown random inputs, *Proceedings of the 14th IMAC*, Dearborn, MI, 1996.
- INPRES-CIRSOC 103 Parte II. Reglamento Argentino para Construcciones Sismo-resistentes de Hormigon Armado; 2000.
- INPRES-CIRSOC 201. Reglamento Argentino de Estructuras de Hormigon Armado; 2000.
- Kawiecki, G. Modal Damping Measurements for Damage Detection, *European COST F3 Conference on System Identification and Structural Health Monitoring*, Madrid, Spain, 651–658, 2000.
- Kim H., Melhem H., Damage detection of structures by wavelet analysis, *Engineering Structures*, 26: 347–362, 2004.
- Lardies J., Gouttebroze S., Identification of modal parameters using the wavelet transform. *International Journal of Mechanical Sciences*, 44: 2263–2283, 2002.
- Lu C.J., Hsu Y.T., Vibration analysis of an inhomogeneous string for damage detection by wavelet transform, *International Journal of Mechanical Sciences*, 44: 745–754, 2002.
- Minh-Nghi Ta, Joseph Lardiès, Identification of weak nonlinearities on damping and stiffness by the continuous wavelet transform. *Journal of Sound and Vibration*, 293: 16–37, 2006.
- Modena, C., Sonda, D., and Zonta, D., Damage Localization in Reinforced Concrete

- Structures by Using Damping Measurements, *Damage Assessment of Structures, Proceedings of the International Conference on Damage Assessment of Structures (DAMAS 99)*, Dublin, Ireland, 132–141, 1999.
- Palazzo, G., Identificación de Sistemas y Evaluación del Daño Estructural, *Master Dissertation* National University of Tucumán, Argentina, 2000.
- Rytter A., Vibration Based Inspection of Civil Engineering Structures, *PhD Thesis*, Aalborg University, Denmark, 1993.
- Salawu OS. Detection of structural damage through changes in frequency: a review. *Engineering Structures*, 19 (9): 718–23, 1997.
- Sohn, H., Farrar, C. R., Hemez, F. M., Shunk, D. D., Stinemates, D. W. and Nadler, B. R., A Review of Structural Health Monitoring Literature: 1996–2001”, *Los Alamos National Laboratory*, USA. 2003
- Takeda, T., M. A., Sozen, and N. Nielsen, "Reinforced Concrete Response to Simulated Earthquakes," *Journal of Structural Division, ASCE*, 96 (ST12), 1970.
- Tang, X., Goel, S. C., "DRAIN-2DM – Technical notes and user's guide," *Research Report UMCE 88-1*, Department of Civil Engineering, University of Michigan at Ann Arbor, MI, 1988.
- Torresani B., *Analyse Continue par Ondelettes*, CNRS Editions, Paris, 1995.
- Wang Q, and Deng X., Damage detection with spatial wavelets, *International Journal of Solids and Structures*, 36: 3443–3468, 1999.
- Zonta, D., Modena, C., and Bursi, O.S., Analysis of Dispersive Phenomena in Damaged Structures, *European COST F3 Conference on System Identification and Structural Health Monitoring*, Madrid, Spain, 801–810, 2000.
- Zou, Y., Tong, L and Steven, G. P., Vibration-based model-dependent damage (delamination) identification and health monitoring for composite structures – a review, *Journal of Sound and Vibration*, 230 (2) : 357-378, 2000.

APPENDIX A THE CONTINUOUS WAVELET TRANSFORM

A.1 Theoretical background

A localized decomposition in the frequency and time domain can be obtained using the continuous wavelet transform. Under assumptions that the function $x(t)$ meets the condition:

$$\int_{-\infty}^{+\infty} |x(t)|^2 dt < \infty \quad (\text{A.1})$$

which implies that $x(t)$ decays to zero at $\pm \infty$, the idea of the continuous wavelet transform is to find a function $g(t)$ which can generate a basis for the entire space of functions $x(t)$. If the decay of this function is very fast, this function is called a small wave or a wavelet. The fast decay introduces locality into the analysis, which is not the case of the Fourier transform where a global representation is obtained. Using a family of basis functions, wavelets can be formulated to describe $x(t)$ in a localized time and frequency format. The continuous wavelet transform gives time and frequency information about the analyzed data. The continuous wavelet transform of the function $x(t)$ is defined as (Chui C.K. ,1992):

$$W_g[x](a,b) = \frac{1}{\sqrt{a}} \int_{-\infty}^{+\infty} x(t) g^* \left(\frac{t-b}{a} \right) dt \quad (\text{A.2})$$

where $g(t)$ is the analyzing or mother wavelet and $g^*(t)$ the complex conjugate of $g(t)$; b is the parameter localizing the wavelet function in the time domain: $W_g[x](a,b)$ shows the local information about $x(t)$ at the time $t = b$ and a is the dilatation or scale parameter defining the analyzing window stretching. The idea of the continuous wavelet transform is to decompose a function $x(t)$ into wavelet coefficients $W_g[x](a,b)$ using the basis of wavelet functions. The wavelet coefficients represent a measure of the similitude between the dilated and shifted wavelet and the function $x(t)$ at time b and scale a . Any function $g(t)$ can be used as an analyzing wavelet if it satisfies the admissibility condition (Chui C.K.,1992):

$$c_g = \int_{-\infty}^{+\infty} \frac{|G(\omega)|^2}{|\omega|} d\omega < +\infty \quad (\text{A.3})$$

where $G(\omega)$ is the *Fourier Transform* of $g(t)$. It follows that $G(\omega)$ is a continuous function, so that the finiteness of c_g implies that $G(0) = 0$, or also that the mean value of $g(t)$ in the time domain is zero. The admissibility condition is necessary to obtain the inverse of the wavelet transform (Chui C.K.,1992). The wavelet $g(t)$ must be also a window function to enable the possibility of time–frequency localization: $g(t)$ decays at infinity, which means that additionally:

$$\int_{-\infty}^{+\infty} |g(t)| dt < \infty \quad (\text{A.4})$$

If it is assumed that $g(t)$ is a rapidly decaying function in time domain, that is the values of $g(t)$ are negligible outside the interval (t_{min}, t_{max}) , the transform becomes local.

It is possible to see the frequency localization when the continuous wavelet transform is expressed in terms of the *Fourier Transform*. Using the *Parseval* identity (Chui C.K.,1992), we can define the frequency domain formulation of the continuous wavelet transform:

$$W_g[x](a,b) = \frac{\sqrt{a}}{2\pi} \int_{-\infty}^{+\infty} X(\omega) G^*(a\omega) e^{j\omega b} d\omega \quad (\text{A.5})$$

This localization depends on the dilatation or scale parameter a .

A number of different analyzing functions have been used in the wavelet analysis. One of the most known and widely used is the complex *Morlet wavelet* defined in the time domain as:

$$g(t) = \frac{1}{\sqrt{2\pi}} e^{-\frac{t^2}{2}} e^{j\omega_0 t} \quad (\text{A.6})$$

where ω_0 is the wavelet central frequency. The dilated version of the *Fourier Transform* is

$$G(a\omega) = e^{-\frac{1}{2}(a\omega - \omega_0)^2} \quad (\text{A.7})$$

In practice the value of ω_0 is chosen $\omega_0 \geq 5$ which meets approximately the requirements given by condition A.3. Note that $G(a\omega)$ is maximum at the central frequency when $a\omega = \omega_0$ and the *Morlet wavelet* can be viewed as a linear band-pass filter whose bandwidth is proportional to $1/a$ or to the central frequency. Thus, the value of the dilatation parameter a corresponding to the pseudo-frequency at which the wavelet filter is focused ω_f , can be determined from $a = \omega_0/\omega_f$.

In summary, the continuous wavelet transform analyses an arbitrary function $x(t)$ only locally at windows defined by a wavelet function. The continuous wavelet transform decomposes $x(t)$ into various components at different time windows and frequency bands. The size of the time windows is controlled by the translation parameter b while the length of the frequency band is controlled by the dilatation parameter a . Hence, one can examine the signal at different time windows and frequency bands by controlling translation and dilatation. However, constrained by the uncertainty principle (Chui C.K., 1992), a compromise usually has to be made choosing either a narrow time windows for good time resolution, or a wide time windows for good frequency resolution. The resolution of the wavelet decomposition in the time-frequency domain is determined by the duration Δt_g and bandwidth Δf_g of the analyzing wavelet and by the value of the dilation parameter a as follow:

$$\Delta t = a \Delta t_g \quad \Delta f = \frac{\Delta f_g}{a} \quad (\text{A.8})$$

The resolution of the analysis is therefore good for high dilation in the frequency domain and for low dilation in the time domain.

A.2 Natural Frequencies and modal damping ratios

Ridge and skeleton of the continuous wavelet transform

Torresani, B. (1995) give the definition of a class of signals called asymptotic and presents some results for the time–frequency analysis of such signals. A signal is asymptotic if the amplitude $A(t)$ varies slowly compared to the variations of the phase. The analytic signal associated with the asymptotic signal is $x_a(t) = A(t) e^{j\varphi(t)}$ and from this definition, the concept of instantaneous angular frequency as the time varying derivative of the phase can be derived: $\omega(t) = \dot{\varphi}(t)$. The continuous wavelet transform of an asymptotic signal $x(t)$ is obtained by asymptotic techniques and can be approximated by (Torresani, B. (1995)):

$$W_g[x](a,b) = \frac{\sqrt{a}}{2} A(b) e^{j\varphi(b)} G^*(a\dot{\varphi}(b)) \quad (\text{A.9})$$

Using the complex *Morlet wavelet*,

$$W_g[x](a,b) = \frac{\sqrt{a}}{2} A(b) e^{j\varphi(b)} e^{-\frac{1}{2}(a\dot{\varphi}(b)-\omega_0)^2} \quad (\text{A.10})$$

The square of the modulus of the continuous wavelet transform can be interpreted as an energy density distribution over the time-scale plane. The energy of the signal is essentially concentrated on the time-scale plane around a region called the *ridge* of the continuous wavelet transform. In other words, the *ridge* of the continuous wavelet transform is the region containing the points defined by $a = a(b)$, where the amplitude of the continuous wavelet transform is maximum. The *ridges* are identified by seeking out the points where the continuous wavelet transform coefficients take on local maximum values: for each value of b ,

we obtain a value as $|W_g[x](a(b),b)| = \max_a W_g[x](a,b)$. To obtain the *ridge*, the dilatation parameter $a = a(b)$ has to be calculated in order to maximize the analyzing wavelet $G^*(a\dot{\varphi}(b))$, that is, using the modified *Morlet wavelet*, for $a = a(b) = \omega_o/\dot{\varphi}(b)$. We obtain:

$$W_g[x](a(b),b) = \frac{\sqrt{a(b)}}{2} A(b) e^{j\varphi(b)} \quad (\text{A.11})$$

The values of the continuous wavelet transform that are restricted to the *ridge* are the *skeleton* of the continuous wavelet transform.

It is important to note that the real components of the continuous wavelet transform along the *ridge* are directly proportional to the signal given by Eq. (1) and from Eq. (A11) we obtain

$$A(b) = 2 \frac{|W_g[x](a(b),b)|}{\sqrt{a(b)}} \quad (\text{A.12})$$

$$\varphi(b) = \text{Arg}(W_g[x](a(b),b)) \quad (\text{A.13})$$

Finally, using the A.12 and A.13 it is possible to estimate the instantaneous amplitude $A(t)$ and the phase $\varphi(t)$. Being the derivative of $A(t)$, $\dot{A}(t)$ and the derivative of $\varphi(t)$, the instantaneous angular frequency $\omega(t) = \dot{\varphi}(t)$, in conjunction with the equations (2), it can be determined the instantaneous undamped natural frequency and damping of the system.